



The Low-Pressure Rheology of Ultra-Thin Lubricant Films and Its Influence on Sliding Contact

J. L. Streator

J. P. Gerhardtstein

C. B. McCollum

George W. Woodruff School of
Mechanical Engineering,
Georgia Institute of Technology,
Atlanta, GA 30332-0405

Lubricant rheology governs the friction in any lubricated contact. In hydrodynamic lubrication, the genesis of friction is well-understood. However, when asperity contacts occur, the situation becomes more complex. In this "mixed" lubrication regime, it is known that lubricants can deviate dramatically from Newtonian behavior, but the source of this effect has not been identified. In particular, the question arises as to whether the non-Newtonian behavior of the lubricant is due to the extreme thinness of the film or to the very large shear rates to which it is subjected. In the current work, we analyze friction force measurements in the magnetic slider/disk interface to help resolve this question. Because of its precision geometry, the slider/disk interface is ideal for such an investigation. Results of the analysis indicate (1) the lubricant retains its bulk viscosity in films as thin as 11–12 molecular diameters; (2) the rheological state of the lubricant is determined by a parameter we introduce here as the "Newtonian" shear stress, and (3) the rheology of the lubricant at high Newtonian shear stress may indicate a newly discovered property of liquids.

1 Introduction

In classical hydrodynamic lubrication, the shear stress is given by the product of viscosity and shear rate. It is therefore a simple matter to determine the friction force. However, when the opposing surfaces are separated by very thin films of lubricant, the situation is more complex. A consideration of the large shear rates encountered with ultra-thin films quickly leads to the conclusion that the lubricant exhibits non-Newtonian behavior. For example, consider a magnetic slider/disk interface that operates with a 10 nm-thick lubricant film¹ having a viscosity of 1 Pa·s. If the relative sliding speed is 1 m/s, the corresponding shear rate is 10^8 s^{-1} and the predicted shear stress is 10^8 N/m^2 . For a bearing area of 3 mm^2 the predicted friction force is 300 N. Such large friction forces are never observed. In fact, to the authors' knowledge, a friction force exceeding 1 percent of this value (i.e., 3 N) has never been reported for the given slider area. Clearly then, the Newtonian model breaks down.

In non-conformal contacts, as in rolling-element bearings, the lubricant experiences large pressures (typically, 10^8 to 10^{10} Pa) and this has motivated investigation of lubricant rheology at high pressure (Bair and Winer, 1979; Bair and Winer, 1982; Hutton, 1985; Evans and Johnson, 1986; Ramesh and Clifton, 1987; Bair and Winer, 1992). These investigations have shown that highly pressurized lubricants exhibit a limiting shear stress

that depends on both temperature and pressure. In contrast there has been relatively little reported in the literature on the rheology of lubricants in conformal contacts which operate at much lower pressures. A lubricant in a typical magnetic slider/disk interface, for example, experiences an average pressure of about 50 kPa if it supports the slider load over the entire bearing area. Lubricants at such low pressure may behave quite differently from what has been observed at high pressure (Winer and Bair, 1987; Bair and Winer, 1992). In the present work, we conduct a detailed analysis of friction force data obtained in a recent study (Streator and Gerhardtstein, 1993) along with some additional measurements for added insight. The purpose of this analysis is to understand the low-pressure rheology of liquid lubricants when applied in very thin films.

2 Experimental

2.1 Test Apparatus. The test apparatus is shown schematically in Fig. 1. The friction force is acquired via a strain gage force transducer. The slider is spring-loaded against the disk by means of the slider suspension. A separate load cell was used to measure the slider load (at the appropriate deflection) prior to placement on the disk. A micrometer stage allows for accurate radial positioning of the slider. The disk is clamped to a servo-controlled spindle which provides good speed control in a low-speed range (0.06 to 60 rpm). The test stand is situated beneath a clean air hood in order to minimize contamination from dust. Data acquisition is accomplished via an A/D card in a personal computer.

2.2 Test Materials. The lubricants used consisted of four branched-chain perfluoropolyether (PFPE) lubricants. Relevant lubricant properties are listed in Table 1. The sliders were

¹Typically, a commercial magnetic disk operates with 1–4 nm of lubricant (Bhushan, 1990). The thickness of 10 nm was chosen for illustration.

Contributed by the Tribology Division of THE AMERICAN SOCIETY OF MECHANICAL ENGINEERS for presentation at the STLE/ASME Tribology Conference, New Orleans, La., October 24–27, 1993. Manuscript received by the Tribology Division March 8, 1993; revised manuscript received June 29, 1993. Paper No. 93-Trib-45. Associate Technical Editor: S. Ioannides.

Copies will be available until March 1995.

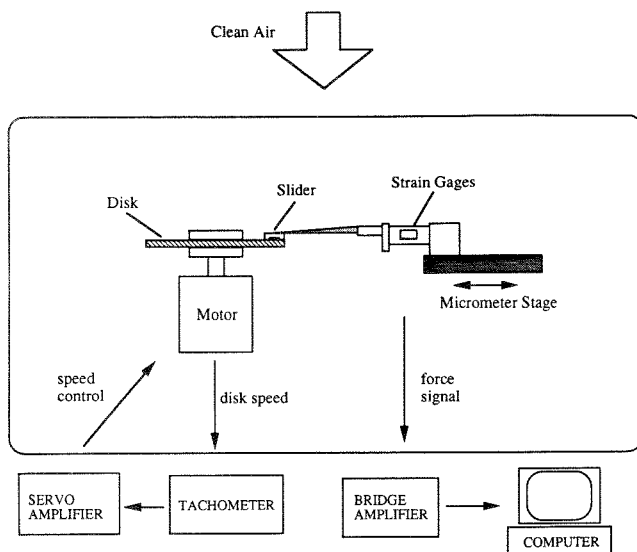


Fig. 1 Schematic of test apparatus

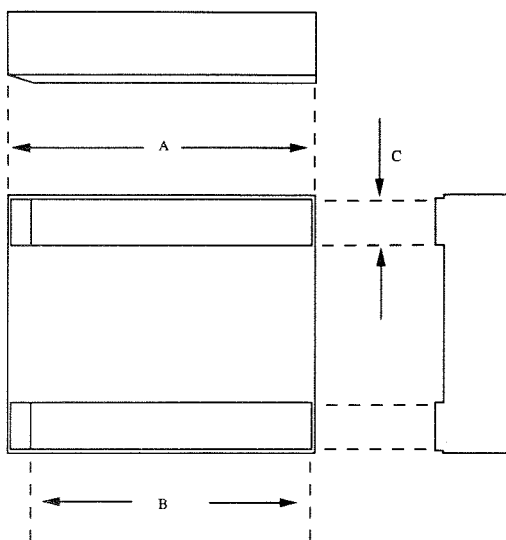


Fig. 2 Slider geometry

ceramic composite sliders made of $\text{Al}_2\text{O}_3\text{-TiC}$. Both "100 percent" and "70 percent" (reduced area) sliders were used in the tests. The overall slider design is illustrated in Fig. 2 and specific slider dimensions are given in Table 2. As observed in Fig. 2, the slider has two rails which, during normal read/write operations of a disk drive, facilitate the development of a hydrodynamic air bearing. According to vendor specifications the slider rails had a positive crown of less than 50 nm.

The disks used for the tests were untextured, 95 mm thin-film magnetic disks with carbon overcoat. The disks were received unlubricated from the vendor. Surface roughness measurements on a sample disk by stylus profilometry yielded a roughness average (Ra) value of approximately 4 nm.

2.3 Test Procedure. Lubricants were applied to the disk using a dip-coating technique described previously (Streator and Johnson, 1992). The dip-coating process involves submerging a disk into a dilute solution of lubricant and then raising it from the bath at a constant speed. The concentration of the lubricant and the rate of withdrawal determine the resulting film thickness (Buttafava et al., 1985; Scarati and Caporiccio, 1987). As the disk emerges from the bath it draws

Table 1 Lubricant properties

| LUBRICANT | DYNAMIC VISCOSITY (Pa-s) (@26°C) | MOLECULAR WEIGHT |
|-----------|----------------------------------|------------------|
| 143AD | 1.96 | 8,250 |
| 143AX | 0.566 | 4,800 |
| 143AY | 0.195 | 3,000 |
| 143AZ | 0.054 | 1,850 |

Table 2 Slider dimensions (see Fig. 2)

| SLIDER TYPE | DIMENSIONS IN mm | | | BEARING AREA (mm ²) |
|-------------|------------------|------|-------|---------------------------------|
| | A | B | C | |
| 100% | 4.06 | 3.81 | 0.381 | 2.9 |
| 70% | 2.84 | 2.59 | 0.254 | 1.3 |

up a certain amount of solution. The volatile solvent, Florinert FC-77, quickly evaporates leaving behind a thin lubricant film. For a given withdrawal rate, the film thickness is proportional to the lubricant concentration (Buttafava et al., 1985). In the present work, lubricant concentration was varied between 0.05 and 2.0 volume percent and the withdrawal rates ranged from 2 to 8 mm/s. With these conditions, lubricants were applied in thicknesses from 23 to 80 nm.

The relationship between lubricant thickness and withdrawal rate was determined via a set of ESCA (Electron Spectroscopy for Chemical Analysis) measurements conducted by an outside vendor. The ESCA data were also used to calibrate measurements obtained via ellipsometry (Hu and Talke, 1988). The ellipsometry measurements were then used to provide rough verification of the target lubricant thickness. To avoid cross-contamination, a single lubricant type was applied to a given disk.

After lubricating the disk to a desired film thickness and performing ellipsometry, the disk was clamped to the spindle. The slider was then loaded to a desired normal force (60 to 280 mN) and the disk was rotated at a desired speed. The friction was sampled for one complete disk revolution. Ten different sliding speeds were investigated: 0.25, 0.55, 1.15, 2.5, 5.5, 11.5, 25, 50, 115 and 250 mm/s. The speeds were varied in either ascending or descending order. Between each lubricant application, the slider was cleaned of any lubricant.

All tests were conducted in ambient temperature (26–29°C) and humidity (19–55% RH).

3 Theoretical

3.1 Hydrodynamic Lubrication. To model the slider/disk interface, we assume the applicability of Reynolds equation and that the lubricant is isoviscous. The validity of the isoviscous assumption is established later. For simplicity we treat the slider and disk surfaces as ideally smooth and flat. In reality both have some degree of roughness and curvature. As seen in Fig. 3, the slider has a short tapered section at the leading edge. However, for the film thicknesses applied (23 to 80 nm) the contact area between the slider and lubricant does not involve the tapered portion. With reference to Fig. 3, the Reynolds equation for each slider rail is given by

$$\frac{\partial}{\partial x} \left(h^3 \frac{\partial p}{\partial x} \right) + \frac{\partial}{\partial z} \left(h^3 \frac{\partial p}{\partial z} \right) = 6\mu U \frac{dh}{dx} \quad (1)$$

Since the width of each slider rail, transverse to the direction of sliding, is much smaller than the rail length (Table 2), we neglect the first term on the right-hand side of (1) in favor of

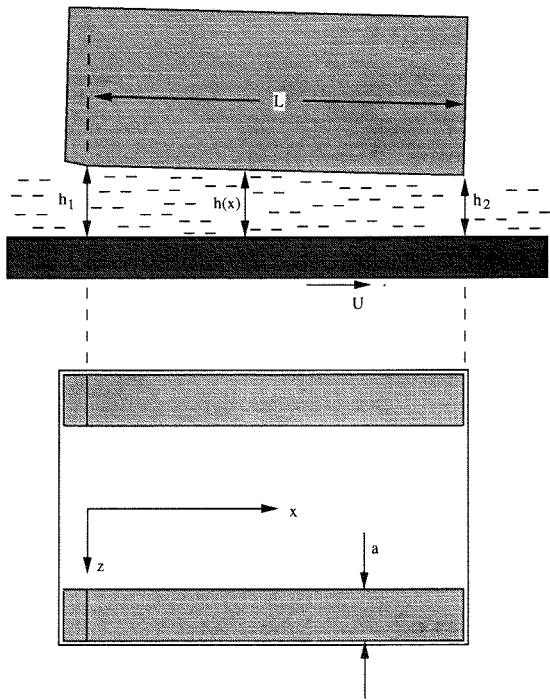


Fig. 3 Schematic of slider/disk interface in hydrodynamic lubrication. Upper portion of figure gives front view of interface. Lower portion gives bottom view of slider.

the second term.² The remaining equation may be solved for the pressure distribution, $p(x, z)$, beneath each rail, yielding

$$p(x, z) = \frac{3\mu U}{h^3} \frac{dh}{dx} (z - z_o)(z - z_o - a) \quad (2)$$

where μ is the dynamic viscosity, U is the sliding speed, h is the film thickness, z_o is the inner-edge location of a given rail, and a is the width of the rail. Integrating over each rail and combining the result, we obtain

$$W_H = \frac{\mu U a^3}{2h^2} \left(1 - \frac{1}{c^2}\right) \quad (3)$$

where W_H is the hydrodynamic load exerted by the film, h_1 and h_2 are the inlet and outlet film thicknesses, respectively (Fig. 3), and $c = h_1/h_2$.

With the assumptions leading to Reynolds equation, the flow field is a combination of Couette and Poiseuille flow, and the shear stress, τ , exerted on the slider is given by

$$\tau = \frac{\mu U}{h} - \frac{h}{2} \frac{\partial p}{\partial x} \quad (4)$$

After making use of (2) in Eq. (4), the (hydrodynamic) friction force, F_H , may be found by integrating the shear stress over each slider rail, yielding

$$F_H = \frac{\mu U A}{h} \left(\frac{\ln c}{c-1} - \frac{3a^2}{8L^2} \frac{(c^2-1)(c-1)}{c^2} \right) \quad (5)$$

where A is the total bearing area, and L is the length of the slider (Fig. 3).

From Eq. (3) we see that the slider must have positive inclination (i.e., $c > 1$) in order to achieve positive load support. For any positive value of inclination it can be shown that the

²The analysis presented here departs from that appearing in Streater and Gerhardtstein (1993), in which the authors assumed one-dimensional flow in the direction of sliding. Owing to the shape of the slider rails, the analysis of the present work is more appropriate and leads to a more accurate estimation of the load capacity of the bearing.

line of action of the hydrodynamic load (i.e., the center of pressure) is to the right of the line of symmetry. For a slider pivoted at its center, the hydrodynamic moment then opposes positive slider inclination. The friction force, F_H , then opposes a moment opposing positive slider inclination. Moreover, any torsional stiffness of the slider at its pivot point acts as a restoring force, resisting positive inclination. Since all of the moments are in the same direction, there is no value of $c > 1$ that satisfies moment balance for the idealized geometry depicted in Fig. 3. We expect, therefore, that the actual slider operates with $c \cong 1$ since load support exists only to the extent that the slider or disk geometries deviate from the ideal (i.e., perfectly smooth and flat).

Further evidence for nearly parallel surfaces (i.e., $c \cong 1$) is obtained by considering typical values of the various operating parameters, such as $W = .15$ N, $\mu = 0.2$ Pa·s, $U = 10$ mm/s, $h_2 = 40$ nm, and $a = 0.381$ mm. Using these values in (3) gives:

$$0.00434 = 1 - \frac{1}{c^2} \quad (6)$$

The above equation is satisfied for $c = 1.0022$. Using the definition of c ($= h_1/h_2$) and recalling $h_2 = 40$ nm, this value of c yields $h_1 - h_2 = 0.09$ nm, which says the two heights differ by atomic distances. Thus the film thickness is constant to the degree that the slider and disk surfaces are smooth and flat.

Using a Taylor's series in (5) and retaining terms of first order in $c-1$, it can be shown that the friction force is approximated by

$$F_H = \frac{\mu U A}{h_2} \left(1 - \frac{c-1}{2}\right) \quad (7)$$

Thus with $c-1 \cong 0$, and $h_1 \cong h_2 \cong h$, we have simply

$$F_H = \frac{\mu U A}{h} \quad (8)$$

3.2 Viscous Heating. The foregoing solution of Reynolds equation, as expressed in (3) and (8), assumed a constant viscosity throughout the film, the validity of which we shall now show. The Energy equation (see, for example, White, 1986) is given by:

$$\rho c_v \frac{DT}{Dt} = k \nabla^2 T + \Phi \quad (9)$$

where ρ is the density, c_v is the specific heat, T is the temperature, t is time, k is the thermal conductivity and Φ is the viscous dissipation function. Assuming steady, Couette flow (see Eq. (8)) with no temperature gradients other than across the film, Eq. (9) reduces to:

$$0 = k \frac{d^2 T}{dy^2} + \Phi \quad (10)$$

where the y -axis is aligned normal to the interface. An upper bound for the viscous dissipation is the square of the velocity gradient multiplied by the viscosity at ambient temperature, which we denote as μ_o . Thus

$$\Phi \leq \mu_o \frac{U^2}{h^2} \quad (11)$$

Integrating (10) and imposing the ambient temperature, T_o , at the walls, we obtain

$$T(y) - T_o \leq \frac{\mu_o U^2}{2kh^2} (hy - y^2) \quad (12)$$

The maximum temperature rise in the film occurs at $y = h/2$, giving

$$\Delta T_{\max} \leq \frac{\mu_o U^2}{8k} \quad (13)$$

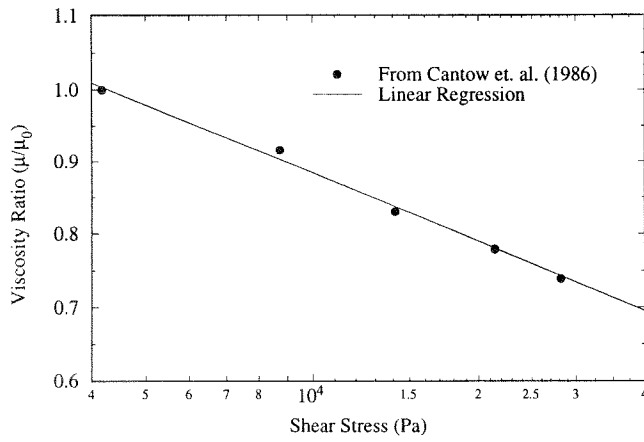


Fig. 4 Shear thinning data of Fomblin YR from Cantow et al. (1986)

The fractional change in viscosity due to the change in temperature is estimated by

$$\frac{\Delta\mu}{\mu_o} \leq \frac{1}{\mu_o} \left. \frac{d\mu}{dT} \right|_{T_o} \Delta T_{\max} = \beta \Delta T_{\max} \quad (14)$$

where β is the viscosity-temperature coefficient of the given lubricant. Combining (13) with (14), yields

$$\frac{\Delta\mu}{\mu_o} \leq \frac{\beta\mu_o U^2}{8k} \quad (15)$$

From vendor specifications, we have, for the highest viscosity lubricant, $\beta = 0.06 \text{ K}^{-1}$, $\mu_o = 2.0 \text{ Pa}\cdot\text{s}$ (@26°C), and $k = 0.09 \text{ W/m}\cdot\text{K}$. Then using $U = 0.25 \text{ m/s}$ (the highest sliding speed used), we obtain

$$\frac{\Delta\mu}{\mu_o} \leq \frac{\beta\mu_o U^2}{8k} = \frac{(0.06)(2)(0.25)^2}{8(0.09)} = 0.01 \quad (16)$$

Therefore the effect of viscous heating on the viscosity is negligible.

3.3 Shear-Thinning. Cantow et al. (1986) investigated the rheology of Fomblin YR at room temperature (25°C) and atmospheric pressure. Fomblin YR, a branched-chain PFPE liquid, is quite similar in structure to the lubricants used in the present study and it is expected to have similar shear-thinning behavior. Results of their measurements are illustrated in Fig. 4 (the data points were actually read from Bhushan (1990) who referenced the above work and provided a more readable graph.) The figure shows the fractional reduction in viscosity as a function of the shear stress. The symbols represent actual measurements, while the solid line is a linear regression of the measured data. Cantow et al. (1986), and Bhushan (1990) presented these data as viscosity versus shear rate, but the form presented in Fig. 4 will prove more convenient for subsequent calculations.

To apply the data of Cantow et al. (1986) to the lubricants of our study, we make the following assumption (Streator and Gerhardtstein, 1993): At the same shear stress, each of the four lubricants experiences the same fractional reduction in viscosity as that of Fomblin YR. The validity of this assumption is investigated later by comparison with experimental measurement. The shear-thinning assumption is expressed mathematically as

$$\frac{\mu}{\mu_o} = r(\tau) \quad (17)$$

where μ is the actual viscosity, μ_o is the nominal or “low-shear” viscosity at the given temperature, τ is the shear stress and $r(\tau)$ is the shear-thinning function plotted in Fig. 4. In its current form, (17) cannot be used to predict the viscosity

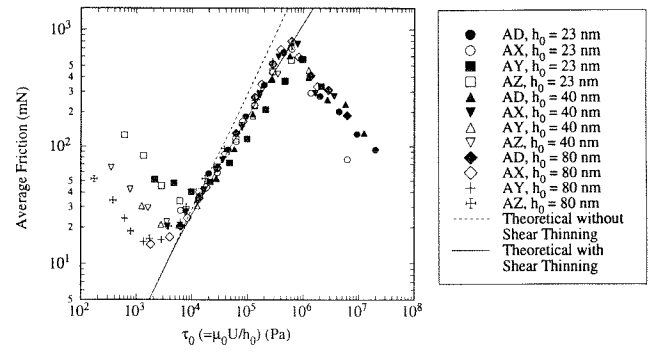


Fig. 5 Friction force versus Newtonian shear stress at three values of the applied lubricant film thickness, h_o , for each of the lubricants. Each data point is the average friction over one disk revolution.

from the operating conditions, since the shear stress is not known *a priori*. We must reformulate (17) to determine the actual viscosity, μ , and the shear stress, τ , from specification of the shear rate. Assuming Couette flow (see Eq. (8)), the shear stress is given by

$$\tau = \frac{\mu U}{h} = \frac{\mu}{\mu_o} \frac{\mu_o U}{h} = r(\tau) \mu_o \frac{U}{h} = r(\tau) \mu_o \dot{\gamma} \quad (18)$$

where $\dot{\gamma}$ is the shear rate. We now define a “Newtonian” shear stress, τ_o as

$$\tau_o = \mu_o \dot{\gamma} \quad (19)$$

This Newtonian shear stress is the shear stress that would result if the lubricant remained Newtonian (i.e., if no shear thinning occurred). From (18) and (19), we obtain

$$\frac{\tau}{\tau_o} = r(\tau) \quad (20)$$

which can be written as

$$\tau_o = \frac{\tau}{r(\tau)} \quad (21)$$

Using the equation for the regression line in Fig. 4 we obtain

$$\tau_o = \frac{\tau}{2.142 - 0.3144 \log_{10} \tau} \quad (22)$$

We can invert (22) numerically to determine the actual shear stress, τ , for a given value of the Newtonian shear stress, τ_o . The viscosity, if needed, may be determined from (17). The predicted (hydrodynamic) friction force, F_H is then given by

$$F_H = \tau A \quad (23)$$

4 Results and Discussion

4.1 Theory Versus Experiment. Figure 5 shows the results of friction measurements for several values of applied lubricant thickness, sliding speed and nominal viscosity. The load was .15 N and the slider area was 2.9 mm². These measurements were reported in Streator and Gerhardtstein (1993)³ but here the data have been normalized with respect to the Newtonian shear stress, τ_o . In calculating τ_o ($=\mu_o U/h_o$), the nominal viscosity was computed using the measured ambient temperature along with viscosity-temperature data supplied by the lubricant vendor. The measured friction data are indicated by the symbols and each data point represents the average friction force over one complete disk revolution. The parameter h_o denotes the *applied* lubricant thickness. The solid line is the theoretical friction force calculated from Eq. (23) and incor-

³In this paper, the slider bearing area was incorrectly reported as 3.1 mm². The correct value is 2.9 mm².

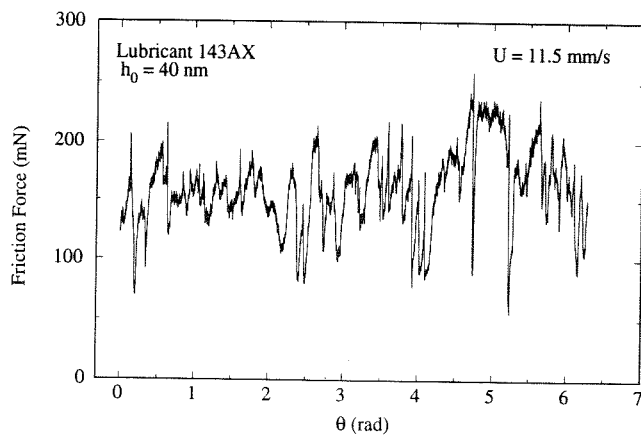


Fig. 6 Friction trace for one disk revolution with 40 nm of Krytox 143 AX. The sliding speed is 11.5 mm/s. The operating conditions correspond to sliding in the hydrodynamic regime.

porates the shear-thinning data of Cantow et al. (1986) (Fig. 4). The dashed line represents the friction force that would result if the viscosity remained constant—that is, with no shear thinning. As observed, the measured friction forces agree well with the theory over a range of Newtonian shear stresses (10^4 to 6×10^5 Pa) when shear thinning is taken into account. With the exception of Krytox 143 AY at 23 nm, all of the measured friction forces are within 20 percent of the theoretical value.⁴ While the disk surface roughness (~ 4 nm) is appreciable compared with the thinnest film (23 nm), the foregoing results suggest that neither surface roughness nor waviness has a significant effect on the average friction force.

Above a Newtonian shear stress value of 10^4 Pa, the friction force data essentially collapse on a single curve. This result suggests that the degree of shear thinning for all lubricants is determined by a single operating parameter, namely the Newtonian shear stress, τ_0 . Moreover, in the range 10^4 Pa $\leq \tau_0 \leq 6 \times 10^5$ Pa, the friction force data validate the earlier assumption that, at the same shear stress, each of the lubricants of the present study experiences the same relative decrease in viscosity as the lubricant (Fomblin YR) studied by Cantow et al. (1986). Outside of the central region of the graph, the measured friction departs dramatically from the predictions of Reynolds equation, the reasons for which will be discussed in later sections.

Figure 6 shows a typical friction trace around the sliding track in the hydrodynamic regime ($10^4 \leq \tau_0 \leq 6 \times 10^5$ Pa). As seen in the graph, the friction force varies considerably around the sliding track. This feature is likely caused by local, dynamic variations in the lubricant film thickness and may be related to surface roughness and/or waviness. Based on ellipsometry data, the applied film thickness showed much smaller variation around the disk.

Returning to Fig. 5, we note that the agreement between theory and experiment in the central part of the graph is evidence that the lubricant retains its bulk, continuum properties in confined films as thin as a few tens of nanometers. This fact is significant when one considers the sizes of the molecules used in the study. For example, Krytox 143 AD, whose molecular structure is shown schematically in Fig. 7, has a number average molecular weight of 8250, corresponding to an average n (Fig. 7) of 48.9. Each monomer unit consists of one C-C and two C-O bonds as part of the chain structure, giving 147 as the number of bonds in the entire molecular chain. Assuming the molecule is in the form of a random coil, we have, following Atkins (1990),

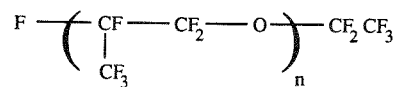


Fig. 7 Chemical structure of Krytox 143 lubricants

$$R_g = l \sqrt{\frac{N}{3}} \quad (24)$$

where R_g is the radius of gyration, l is the average bond length, and N is the number of bonds in the chain. Using $N=147$ and $l=0.14$ nm (Lide, 1992), we obtain $R_g=0.98$ nm. Taking $2R_g$ as a representative molecular diameter, we obtain 2.0 nm as the approximate thickness of a single molecular layer. In Fig. 5, the thinnest film tested was 23 nm, which, based on the given molecular size, corresponds to about 11–12 molecular diameters. To the authors' knowledge, this is the smallest number of layers for which a liquid's bulk viscosity has been observed in simple, Couette flow. On the other hand, previous studies with squeeze films in the surface force apparatus (SFA) (Chan and Horn, 1985; Israelachvili, 1986; Israelachvili and Kott, 1989) have reported bulk behavior with films as thin as 10 molecular layers. Couette-type measurements with the SFA have also been performed, but these have occurred with films consisting of less than 7 molecular layers and have indicated that the effective viscosity may be enhanced by several orders of magnitude with films this thin (Israelachvili et al., 1988; Israelachvili and Kott, 1989; Gee et al., 1990; Granick et al., 1991). Nevertheless, extrapolation of these results to thicker films suggests that bulk behavior should be recovered when the film thickness reaches about 10 molecular layers—at least for the types of molecules investigated (Israelachvili et al., 1988; Israelachvili and Kott, 1989).

4.2 Mixed Lubrication. For Newtonian shear stresses, τ_0 , less than about 4×10^3 Pa (Fig. 5) the measured friction force deviates considerably from the theoretical prediction, showing greater deviation at lower values of the Newtonian shear stress. In some cases, the friction force exceeds that of an unlubricated interface, which is about 40–50 mN (see Fig. 11). The source of these effects is discussed below.

In any given sliding test, the external load, W , is constant and is, in the hydrodynamic regime, equal to W_H of Eq. (3). Within the hydrodynamic regime, the lubricant thickness, h , is equal to the applied thickness, h_0 . Therefore, as the speed, U , is decreased, the value of c must increase to maintain $W_H=W$. (The viscosity, μ , changes somewhat due to shear-thinning, but does not vary nearly enough to compensate for a large reduction in U .) Since c is very close to 1 (see section 3.1), a slight increase in c can change W_H by a large factor. For example, if c increases from 1.0001 to 1.001, W_H increases by a factor of ten (Eq. (3)), thereby accommodating a factor of 10 decrease in U for a fixed load. However, as noted earlier, with an ideally flat slider and disk, there is no finite value of c consistent with moment equilibrium. Hence there is a minimum speed, U , for which c will have reached the maximum value attainable for the slider/disk separation at the applied film thickness. Below this value of U , the actual film thickness, h , must decrease below the applied thickness, h_0 . At sufficiently low speeds, the hydrodynamic load, W_H , is incapable of supporting the external load and the slider comes into contact with the disk.⁵

Both full-film conditions and slider/disk contact may occur within a given revolution of the disk. Figure 8 shows the friction

⁴For each experimental run, the disk speeds were varied in descending order. Comparison measurements taken in ascending order exhibited similar trends but with more spread in the data.

⁵Here we define "contact" as the development of isolated regions of high pressure (i.e., at surface peaks). However, contact does not imply complete penetration of the lubricant film. It is possible that a monolayer of lubricant remains between the slider and disk at their points of closest approach.

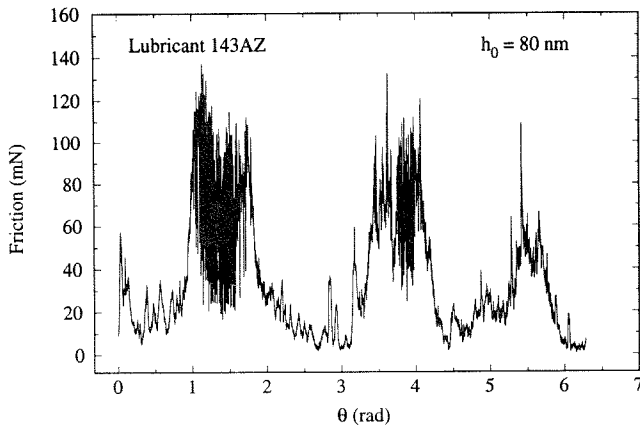


Fig. 8 Friction trace for one disk revolution with 80 nm of Krytox 143 AZ. The sliding speed is 0.25 mm/s. The operating conditions correspond to sliding in the mixed lubrication regime.

trace over one revolution of the disk for 80 nm of Krytox 143 AZ with the reduced-area slider (Table 2) and a sliding speed of 0.25 mm/s. The sliding condition gives a Newtonian shear stress value, τ_o , equal to 170 Pa which, from Fig. 5, represents an operating point well into the mixed regime. The large variations in friction force observed in Fig. 8 are caused by repeated transitions from full-film conditions to instances where appreciable load is borne by the asperities. The lowest friction force observed (1.3 mN) is consistent with full-film lubrication: if we assume an average height, h , of 12 nm, where the slider just clears the asperities, the average shear rate will be about $21,000 \text{ s}^{-1}$, and the predicted friction force (23), assuming Newtonian behavior, will be 1.5 mN, showing excellent agreement.

The data of Fig. 8 also include friction forces greatly in excess of the lowest values. The increase in friction above the minimum points indicates transfer of load from the lubricant film to the asperity contacts. This process can be seen more clearly by considering the balance of forces in the mixed regime (Fig. 9):

$$W_H + W_s = W + W_a \quad (25)$$

where W_H is the hydrodynamic lift, W_s is the load supported by the asperity contacts, W is the external load, and W_a is the adhesive force. The hydrodynamic lift, W_H , should be reasonably approximated by (3) even when the slider and disk surfaces are in contact,⁶ although $c (= h_1/h_2)$ would be difficult to pin down. The adhesive force, W_a , which may be attributed to capillary effects or to intermolecular attraction (Stanley et al., 1990), acts as an additional external load in the interface (Matthewson and Mamin, 1988). As of yet there is no theory which provides the value of W_a in a dynamic contact. There is some evidence, however (Streator et al., 1991; Streator and Johnson, 1992), that W_a depends both on the sliding speed and on the applied lubricant film thickness.

With reference to Fig. 9, the friction force, F , is given by

$$F = F_H + F_s \quad (26)$$

where F_H is the tangential force contributed by the lubricant and F_s is the friction force sustained at the asperity contacts. Assuming Couette flow, F_H , is given by (8), where h represents an average film thickness. At the asperity tips, we expect no

⁶Since the interface is rough, there will be an average slider/disk spacing of about 10 nm even when the two surfaces are in contact. The analysis presented here assumes that the bulk viscosity is not changed when the film is 10 nm thick. This assumption seems reasonable for the Krytox 143 AZ which, owing to its smaller molecular weight (1,850) has a smaller molecular diameter (~ 0.9 nm). Thus a 10 nm-thick film represents 11 molecular layers and this many layers of Krytox 143 AD (i.e., 23 nm) was shown to exhibit bulk behavior (Fig. 5).

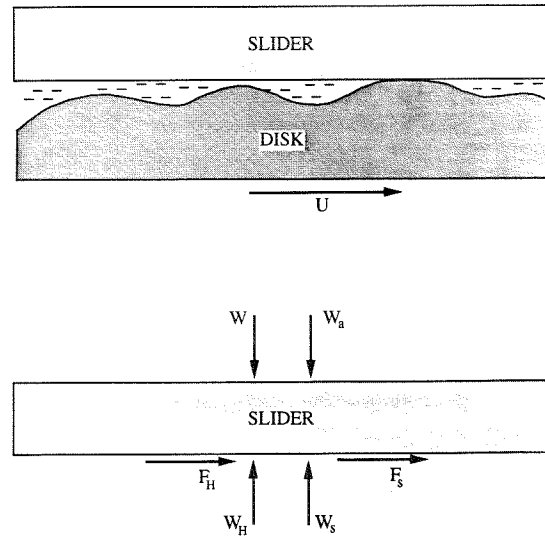


Fig. 9 Force balance in the mixed lubrication regime (see text for definitions of terms)

more than a monolayer or so of lubricant and it has been shown (Streator et al., 1991) that the friction coefficient is virtually unchanged by such a thin film. Thus,

$$F_s = f W_s = f (W + W_a - W_H) \quad (27)$$

where f is the unlubricated friction coefficient. Using (3), (8), (26) and (27) we arrive at

$$F = \frac{\mu U}{h} A + f \left[W + W_a - \mu U \frac{a^3}{2h^2} \left(1 - \frac{1}{c^2} \right) \right] \quad (28)$$

When slider/disk contact is maintained so that the film thickness, h , is minimal (about 10 nm), it is seen from (28) that the friction force, F , depends on the product of velocity and viscosity. Assuming that, on average, c and W_a are independent of the product μU , Eq. (28) suggests that the friction force, F , should normalize with respect to μU in the mixed lubrication regime. This feature is evident in Fig. 5 for each value of the applied lubricant thickness (23, 40 and 80 nm). Equation (28) also predicts that, as the speed and viscosity are decreased, the hydrodynamic effects diminish, whereby the friction force approaches the product of the unlubricated friction coefficient, f , and the effective load, $W + W_a$. Since, in Fig. 5, the three curves separate according to the applied lubricant thickness, h_o , it suggests that W_a is a function of this quantity. The adhesive force is evidently sensitive to the amount of liquid at the periphery of the interface. When the interface is "flooded," the adhesive force is small (Streator et al., 1988; Streator and Gerhardstein, 1993), but when there is just enough liquid to cover the interface, strong adhesion occurs (Yanagisawa, 1985; Matthewson and Mamin, 1988).

4.3 Lubricant Rupture. At a Newtonian shear stress of about 6×10^5 Pa (Fig. 5), the friction force achieves a maximum. Following Winer and Bair (1987) and Bhushan (1990), it was proposed (Streator and Gerhardstein, 1993) that this peak in the friction was evidence of lubricant rupture. Given a shear stress, τ , and pressure, p , it can be shown that the maximum principal stress, σ_I , is given by

$$\sigma_I = \tau - p \quad (29)$$

If we assume that σ_I is limited by some tensile strength, σ_m , of the lubricant, then we have from (29)

$$\tau_{\max} = p + \sigma_m \quad (30)$$

For the data of Fig. 5, the average pressure is 0.052 MPa and the maximum shear stress is 0.28 MPa. From (30) this gives $\sigma_m = 0.23$ MPa. However, this value corresponds to the average

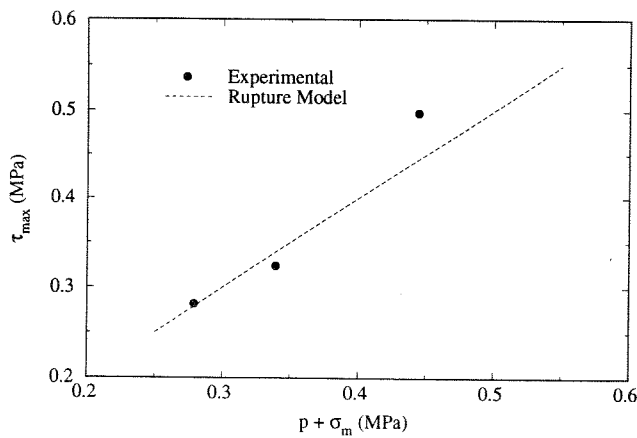


Fig. 10 Comparison of lubricant rupture model with experimental data

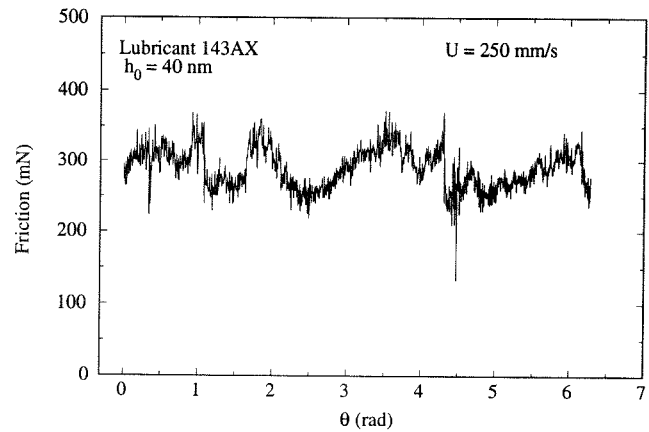


Fig. 12 Friction force trace for one disk revolution with 40 nm of Krytox 143 AX. The sliding speed is 0.25 m/s. The operating conditions yield a Newtonian shear stress of 3.0×10^6 Pa, corresponding to the rupture regime (Fig. 5).

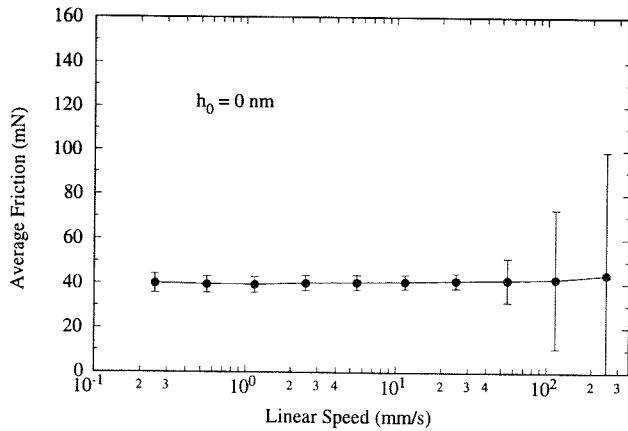


Fig. 11 Friction force versus sliding speed on an unlubricated disk

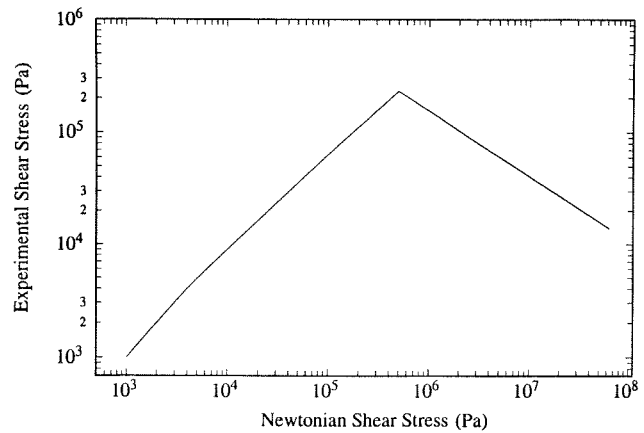


Fig. 13 Rheological behavior of lubricants (based on data of Fig. 5)

shear stress around one disk revolution. The maximum observed shear stress over the sliding track would be a more appropriate measure of the limiting tensile strength. In a recent paper (Streator, 1993), a value of $\sigma_m = 0.3$ MPa was used with considerable success in predicting upper bounds for stiction in the magnetic slider/disk interface.

Equation (30) predicts that the maximum shear stress depends linearly on the contact pressure, assuming the lubricant tensile strength itself is insensitive to pressure. Figure 10 shows the limiting shear stress (averaged around one disk revolution) plotted against the quantity, $p + \sigma_m$. The data were obtained from friction measurements with the reduced-area slider (Table 2) at varying load (60, 140, and 280 mN). Each data point is the average of two separate measurements. The dashed line shows the prediction from (30) where we have used $\sigma_m = 0.23$ MPa, from above. Reasonable agreement is found between the predicted maximum shear stress and the experimental data.

At values of Newtonian shear stress exceeding the point of lubricant rupture, the lubricant experiences dramatic shear thinning (Fig. 5). Because the friction remains normalized with respect to the Newtonian shear stress, the data of Fig. 5 suggests that full-film conditions are still maintained at the applied film thickness, h_o , within this rupture regime.

Since the sliders used in the present study are designed to fly on an air bearing, the question may arise as to whether the friction reduction at the higher speed can be attributed to the slider beginning to take off. Figure 11 shows friction force versus sliding speed under unlubricated conditions for the entire range of speeds used in the present work. The “error” bars indicate one standard deviation above and below the mean in the friction signal. The increase in the size of the error bars

at the higher sliding speeds indicates friction-induced vibration (Streator and Bogy, 1992). As indicated in the figure, the average friction force is virtually unchanged up to the highest sliding speed, indicating full slider-disk contact.

Further evidence for the lack of a transition to a hydrodynamic air bearing is indicated in Fig. 12. This figure shows the friction record for one disk revolution in the case of 40 nm of lubricant 143 AX at a sliding speed of 0.25 m/s, taken at a temperature of 28.7°C. These operating conditions yield a Newtonian shear stress of 3.0×10^6 Pa and therefore correspond to a data point in the regime of decreasing friction (Fig. 5). Since the friction remains high for the complete revolution, there are no instances where the slider is supported by an air bearing.

Another possible explanation for the reduction in friction force at the higher speeds is that slip occurs at the slider/lubricant interface at high values of Newtonian shear stress. However, in the case of slip, one would not expect the friction force to normalize with respect to the same parameter (τ_o) that governs the shear-thinning behavior at lower values of Newtonian shear stress (Fig. 5).

Figure 13 shows the dependence of actual shear stress on Newtonian shear stress for the four lubricants investigated. Below the rupture point, the curve is based on the inversion of (22). Beyond the rupture point, the curve is a linear regression through the experimental data of Fig. 5. We propose that Fig. 13 characterizes the rheological behavior of this class of lubricants.

4.4 Explanation of Previous Friction Measurements. The rheological curve (Fig. 13) helps to explain some puzzling results of previously acquired friction force data. Streator et al. (1991) measured the dynamic friction in a slider/disk interface lubricated with several PFPE liquids. In one set of tests (see Fig. 5c in the above reference) the friction force was found to decrease significantly as the sliding speed was increased. In the above named paper, this behavior was attributed to a time-dependent adhesion mechanism. However, the results of the current test suggest this drop in friction arises from the rheological behavior of Fig. 13. To illustrate: the friction with lubricant "L1" (Fomblin Z03) decreased from 0.53 N to 0.11 N⁷ when the sliding speed was increased from 0.12 m/s to 1.2 m/s. At the mean temperature used in the test (25°C) the viscosity of Fomblin Z03 is 0.043 Pa·s. The applied film thickness was 6 nm. Since the disk used was very smooth (about 2 nm Ra), it is conceivable that this film thickness achieved full-film conditions. At 0.12 m/s the Newtonian shear stress was then 8.6×10^5 Pa which predicts an actual shear stress of 1.6×10^5 Pa according to Fig. 13. This value yields a predicted friction force of 0.46 N, given the slider area⁸ of 2.9 mm². This result compares well with the measured friction (0.53 N). At 1.2 m/s the Newtonian shear stress was 8.6×10^6 Pa and the predicted shear stress (Fig. 13) is 4.1×10^4 Pa, yielding a predicted friction force of 0.12 N. Again good agreement is found with the experimental value (0.11 N). Apparently, even this 6 nm-thick film of Fomblin Z03 exhibits bulk, continuum behavior.

5 Conclusions

Friction measurements were performed in the slider/disk interface with several perfluoropolyether lubricants at lubricant thicknesses ranging from 23 to 80 nm. The friction data were compared with the solution of Reynolds equation for a two-dimensional slider bearing. Several important observations were made:

1. The measured viscosity of the lubricant was indistinguishable from its bulk value in films as thin as 23 nm. In the case of the highest molecular weight lubricant, this thickness represented 11–12 molecular diameters.
2. The rheological state of all lubricants was determined by a single operating parameter introduced here as the "Newtonian" shear stress. The Newtonian shear stress is the product of the shear rate and the nominal, or low-shear, viscosity.
3. At high values of *Newtonian* shear stress, the actual shear stress peaks and then decreases dramatically with increasing shear rate for a given lubricant. This rheological behavior, evidently reported here for the first time, may indicate a newly found property of liquids.

The foregoing results have implications for a number of tribological systems. Low-pressure, conformal contacts (i.e., journal bearings, piston-cylinders, etc.) often operate in a mixed lubrication regime. The observations of the present study suggest that the friction in these systems may be governed by the bulk, continuum behavior of the lubricant rather than by properties specific to ultra-thin films.

Acknowledgments

This work was supported by the National Science Foundation through Grant No.'s MSS-9110469 and MSS-9258014. The authors would like to thank IBM Corporation for donating some of equipment used in the tests. Finally, one of the authors (J.S) would like to thank Drs. Scott Bair and Ward Winer for their insightful comments.

⁷The load was not reported, but was 0.15 N as in the present study.

⁸The slider area was not reported in Streator et al. (1991), but the slider type was the same as 100 percent sliders used in the present study.

References

- Atkins, P. W., 1990, *Physical Chemistry*, W. H. Freeman and Co., New York.
- Bair, S., and Winer, W. O., 1979, "Shear Strength Measurements of Lubricants at High Pressure," *ASME JOURNAL OF LUBRICATION TECHNOLOGY*, Vol. 101, No. 3, pp. 251–257.
- Bair, S., and Winer, W. O., 1982, "Some Observations in High Pressure Rheology of Lubricants," *ASME JOURNAL OF LUBRICATION TECHNOLOGY*, Vol. 104, No. 3, pp. 357–364.
- Bair, S., and Winer, W. O., 1992, "The High Pressure High Shear Stress Rheology of Liquid Lubricants," *ASME JOURNAL OF TRIBOLOGY*, Vol. 114, No. 1, pp. 1–13.
- Bhushan, B., 1990, *Tribology and Mechanics of Magnetic Storage Devices*, Springer-Verlag, New York.
- Buttafava, P., Bretti, V., Ciardello, G., Piano, M., Caporiccio, G., and Scarati, A. M., 1985, "Lubrication and Wear Problems of Perpendicular Recording Thin Flexible Media," *IEEE Trans. Magn.*, Vol. 21, pp. 1533–1535.
- Cantow, M. J. R., Ting, T. Y., Barrall, E. M., Porter, R. S., and George, E. R., 1986, "Shear Dependence of Viscosity for Perfluoropolyether Fluids," *Rheo. Acta.*, Vol. 25, pp. 69–71.
- Chan, D. Y. C., and Horn, R. G., 1985, "The Drainage of Thin Liquid Films Between Solid Surfaces," *J. Chem. Phys.*, Vol. 83, No. 10, pp. 5311–5324.
- Evans, C. R., and Johnson, K. L., 1986, "The Rheological Properties of EHD Lubricants," *Proc. Instn. Mech. Engrs.*, Vol. 200, No. C5, pp. 303–312.
- Gee, M. L., McGuiggan, P. M., and Israelachvili, J. N., 1990, "Liquid to Solidlike Transitions of Molecularly Thin Films Under Shear," *J. Chem. Phys.*, Vol. 93, No. 3, pp. 1895–1906.
- Granick, S., 1991, "Motions and Relaxations of Confined Liquids," *Science*, Vol. 253, pp. 1374–1379.
- Hu, Y., and Talke, F. E., 1988, "A Study of Lubricant Loss in the Rail Region of a Magnetic Recording Slider Using Ellipsometry," *Tribology and Mechanics of Magnetic Storage Systems*, STLE SP-25, Vol. V, pp. 43–48.
- Hutton, J. F., 1985, "Re-Assessment of Rheological Properties of LVI 260," *ASME JOURNAL OF LUBRICATION TECHNOLOGY*, Vol. 106, pp. 536–537.
- Israelachvili, J. N., 1986, "Measurement of the Viscosity of Liquids in Very Thin Films," *J. Coll. Inter Sci.*, Vol. 110, No. 1, pp. 263–271.
- Israelachvili, J. N., and Kott, S. J., 1989, "Shear Properties and Structure of Simple Liquids in Molecularly Thin Films: The Transition from Bulk (Continuum) to Molecular Behavior with Decreasing Film Thickness," *J. Coll. Inter. Sci.*, Vol. 129, No. 2, pp. 461–467.
- Israelachvili, J. N., McGuiggan, P. M., and Homola, A. M., 1988, "Dynamic Properties of Molecularly Thin Liquid Films," *Science*, Vol. 240, pp. 189–191.
- Lide, D. R., ed., 1992, *CRC Handbook of Chemistry and Physics*, CRC Press, Boca Raton, 73rd edition.
- Matthewson, M. J., and Mamin, H. J., 1988, "Liquid Mediated Adhesion of Ultra-Flat Solid Surfaces," *Proc. Mat. Soc. Symp.*, Vol. 119, pp. 87–92.
- Ramesh, K. T., and Clifton, R. J., 1987, "A Pressure Shear Plate Experiment for Studying the Rheology of Lubricants at High Pressure and High Shearing Rates," *ASME JOURNAL OF TRIBOLOGY*, Vol. 109, No. 2, pp. 215–222.
- Scarati, A. M., and Caporiccio, G., 1987, "Frictional Behavior and Wear Resistance of Rigid Disks Lubricated with Neutral and Functional Perfluoropolyethers," *IEEE Trans. Magn.*, Vol. 23, pp. 106–108.
- Stanley, H. M., Etsion, I., and Bogy, D. B., 1990, "Adhesion of Contacting Rough Surfaces in the Presence of Sub-Boundary Lubrication," *ASME JOURNAL OF TRIBOLOGY*, Vol. 112, pp. 98–104.
- Streator, J. L., 1993, "Modeling Stiction in Liquid-Lubricated Slider-Disk Contacts," *Adv. Inf. Stor. Sys.*, Vol. V, ASME Press, New York, in press.
- Streator, J. L., and Bogy, D. B., 1992, "Accounting for Transducer Dynamics in the Measurement of Friction," *ASME JOURNAL OF TRIBOLOGY*, Vol. 114, No. 1, pp. 86–94.
- Streator, J. L., Bhushan, B., and Bogy, D. B., 1991, "Lubricant Performance in Magnetic Thin Film Disks with Carbon Overcoat—Part I: Dynamic and Static Friction," *ASME JOURNAL OF TRIBOLOGY*, Vol. 113, No. 1, pp. 22–31.
- Streator, J. L., Etsion, I., and Bogy, D. B., 1988, "The Effect of Lubrication on the Static and Low-Speed Dynamic Friction in Thin Film Magnetic Disks," *Tribology and Mechanics of Magnetic Storage Systems*, STLE SP-25, Vol. V, pp. 24–29.
- Streator, J. L., and Gerhardstein, J. P., 1993, "Lubrication Regimes for Nanometer-scale Lubricant Films with Capillary Effects," Proceedings of the 19th Leeds-Lyon Symposium on Tribology, "Thin Films in Tribology," D. Dowson, C. M. Taylor, M. Godet, and D. Berthe, eds., Elsevier, New York, in press.
- Streator, J. L., and Johnson, J. K., 1992, "Velocity-Dependent Adhesion with Lubricants on Thin-Film Disks," *Tribology and Mechanics of Magnetic Storage Systems*, STLE SP-35, Vol. VIII, pp. 67–73.
- White, F. M., 1986, *Fluid Mechanics*, McGraw-Hill, New York.
- Winer, W. O., and Bair, S. S., 1987, "The Influence of Ambient Pressure on the Apparent Shear Thinning of Liquid Lubricants—An Overlooked Phenomenon," Paper No. C190/87, *Int. Mech. Engrs. (Lond.)*, pp. 395–398.
- Yanagisawa, M., 1985, "Lubricants on Plated Magnetic Recording Disks," *Tribology and Mechanics of Magnetic Storage Systems*, STLE SP-19, Vol. II, pp. 16–20.